In utero treatment of myelomeningocele with allogenic umbilical cord-derived mesenchymal stromal cells in an ovine model

Lucie Guilbaud, Anaïs Dugas, Mathilde Weber, Carole Deflers, Pauline Lallemant, Thomas Lilin, Clovis Adam, Audrey Cras, Miryam Mebarki, Michel Zérah, et al.

Version of Record: https://www.sciencedirect.com/science/article/pii/S2452318621000404
Manuscript_86928cf5d01d47727e46e6dd5abb9bf7

In utero treatment of myelomeningocele with allogenic umbilical cord-derived mesenchymal stromal cells in an ovine model

Guilbaud L.[1,2,3,4], Dugas A.[1,2,3,4], Weber M.[1,2], Deflers C.[1,2], Lallemant P.[4,5], Lilin T.[6], Adam C.[7], Cras A.[1,8], Mebarki M.[1,2], Zérah M.[4,9], Faivre L.[1,2], Larghero J.[1,2], Jouannic JM.[3,4]

1. Université de Paris, AP-HP, Hôpital Saint-Louis, Unité de Thérapie Cellulaire et Centre MEARY de Thérapie Cellulaire et Génique, Paris, France
2. Stem Cell Biotechnologies, U976 et Centre d'Investigation Clinique en Biothérapies CIC-BT CBT501, INSERM, Paris, France
3. Sorbonne University, AP-HP, Trousseau Hospital, DMU ORIGYNE, Department of Fetal Medicine, Paris, France.
4. National Reference Center for Rare Disease: Vertebral and Spinal Cord Anomalies (MAVEM Center), AP-HP, Trousseau Hospital, Paris, France
5. Sorbonne University, AP-HP, Trousseau Hospital, Department of Physical Medicine and Rehabilitation, Paris, France.
6. Center for Biomedical Research, National Veterinary School, Maisons Alfort, France.
7. Paris Saclay University, Kremlin Bicêtre Hospital, Department of Pathology, Le Kremlin-Bicêtre, France.
8. Université de Paris, Innovative Therapies in Haemostasis, UMR1140 and Centre d'Investigation Clinique en Biothérapies CIC-BT CBT501, INSERM, Paris, France
9. Paris University, AP-HP, Necker Enfants Malades Hospital, Department of Pediatric Neurosurgery, 149 Rue de Sèvres, 75015 Paris, France.

GUILBAUD Lucie (Corresponding Author)

Phone number: +33 6 31 82 32 71

Fax number: +33 1 44 73 51 27

Email address: lucie.guilbaud@aphp.fr

Mail address: : Service de Médecine fœtale, Hôpital Armand Trousseau, APHP, 26 avenue du Docteur Arnold Netter 75012 Paris, France

In utero treatment of myelomeningocele with allogenic umbilical cord-derived mesenchymal stromal cells in an ovine model

Summary

Purpose of the study: The purpose of our study was to investigate the effects of ovine umbilical cord-derived mesenchymal stromal cells (UC-MSCs) seeded in a fibrin patch as an adjuvant therapy for fetal myelomeningocele repair in the ovine model.

Materials and methods: MMC defects were surgically created at 75 days of gestation and repaired 15 days later with UC-MSCs patch or an acellular patch. At birth, motor function, tail movements, and voiding abilities were recorded. Histological and immunohistochemical analysis included study of MMC defect's healing, spinal cord, UC-MSCs survival, and screening for tumors.

Results: Six lambs were born alive in each group. There was no difference between the two groups on the median sheep locomotor rating score but all lambs in the control group had a score between lower than 3 compared to 50% in UC-MSCs group. There were more lambs with tail movements and voiding ability in UC-MSCs group (83% vs 0% and 50% vs 0%, respectively). Grey matter area and large neurons density were higher in UC-MSCs group (2.5 vs 0.8 mm^2 and 19.3 vs 1.6 neurons/mm^2 of gray matter, respectively). Fibrosis thickness at the myelomeningocele scar level was reduced in UC-MSCs group (1269µm vs 2624µm). No tumors were observed.

Conclusion: Fetal repair of myelomeningocele using allogenic UC-MSCs patch provides a moderate improvement in neurological functions, gray matter and neuronal preservation and prevented from fibrosis development at the myelomeningocele scar level.

Key words: myelomeningocele, spina bifida, mesenchymal stromal cells, umbilical cord, ovine model, fetal surgery, fetal stem cell

1. Introduction

Myelomeningocele (MMC) is the most frequent neural tube defect prenatally diagnosed. This malformation leads to lifelong disabilities including lower extremity paralysis, sphincters deficiency, sexual dysfunction, and cognitive disabilities. The Management of Myelomeningocele (MOM) study demonstrated the benefits of prenatal surgery for MMC on motor function [1]. Since then, several centers around the world have been offering this fetal surgery, with similar results to the MOM study [2-5]. The follow-up of the MOM study's children at school-age demonstrates that motor improvement achieved after fetal surgery still exists over the years [6]. However, this benefit remains limited since 71% of children are not able to walk independently at an average age of 7.8 years. In addition, fetal surgery does not seem to provide an improvement in sphincter functions [7,8]. Therefore, it seems necessary to develop adjuvant therapies to fetal surgery in order to improve fetal spinal cord repair and children's prognosis. Stem cell therapy seems to be a relevant option.

Mesenchymal stromal cells (MSC) are multipotent cells that have been isolated from a variety of tissues including bone marrow, adipose tissue, dental tissue, amniotic fluid, placenta and umbilical cord [9,10]. Among MSCs, those from fetal tissue are particularly interesting because they are easy to isolate, have excellent proliferative potential, faster growth rate and lower immunogenicity compared to adult MSCs from bone marrow or adipose tissue [11-13]. It has been demonstrated that the secretome of MSCs isolated from umbilical cords (UC-MSCs) has proangiogenic, antiapoptotic and immunomodulatory effects as well as properties to stimulate endogenous repair, neurogenesis and neuroprotection [14]. Moreover, interest of using UC-MSCs in spinal cord injuries has been demonstrated in numerous animals and human studies [15-20].

The purpose of our study was to investigate the effects of allogenic ovine UC-MSCs seeded in a fibrin patch as an adjuvant therapy for fetal MMC repair in the ovine model.

2. Materials and methods

2.1. Ethics statement

This study protocol was approved by the French national committee on animal research (APAFIS#2845-2015100520053611v10) and all animals received care in strict compliance with institutional guidelines, and guidelines for the provision of standard care to laboratory animals.

2.2. Isolation, expansion, and Green Fluorescent Protein transduction of ovine UC-MSCs

Five umbilical cords were collected from lambs delivered by cesarean section at 139 days of gestation (full term: 142 days) and UC-MSCs were isolated using the explant method. Briefly, the UC was rinsed in saline solution and a longitudinal incision was performed in order to remove the two arteries and two veins. The cord was then cut into pieces of 5 mm of length, placed into 6-well plates (Corning, New York, USA) with complete medium composed of Mimimum Essential Medium alpha (MEM α) GlutaMAX™ supplement, no nucleosides (Gibco, Life technologies, Paisley, UK), supplemented with 10% of Fetal Bovine Serum (FBS, Biowest, Nuaille, France) and 1% antibiotic-antimycotic (Gibco, Life technologies, Grand Island, USA). The plates were kept in a humidified incubator at 37°C and 5% CO_2. The complete medium was changed every day during 4 to 5 days, until cells migrate to the well bottom and the cord explants could be removed. Thereafter, the medium use to feed expanding cells was changed every 3 to 4 days. Morphology of isolated cells was assessed every day, using an inverted microscope. Adherent cells were detached once they reached 90% confluence, using 0.25% Trypsin 0.05 mM EDTA (Gibco, Life technologies, Grand Island, USA) for 5 minutes at 37°C. Isolated cells were pelleted by centrifugation (400xg, 5 min) counted using Trypan Blue (Gibco, Life technologies, Grand Island, USA) exclusion in a KOVA® Glasstic® slide (Garden Grove, USA). The isolated cells were expanded as a monolayer. The cells were cultured with a seeding density of 5000 cells/cm^2

in complete medium, changed every 3 to 4 days. Once the cells reach about 80-90% confluence, cells were trypsinized and counted.

UC-MSCs were transduced with a green fluorescent protein (GFP)-containing lentiviral vector (Dharmacon™ GIPZ™ Lentiviral shRNA, Horizon Discovery, Lafayette, USA). At the end of passage 1, cells were plated at a density of 15 000 cells/cm^2 with serum-free growth medium and allowed to adhere overnight. The next day (day 1), the medium was removed, and the lentiviral particles were added to achieve a multiplicity of infection of 10. Six hours post-transduction, complete medium was added to the cells before an overnight incubation. On day 2, medium was changed, and the cells were examined using fluorescent microscopy to confirm the presence of the reporter gene (TurboGFP). Cells selection was conducted using puromycin (10µg/mL) over a period of approximately 10 days. After selection, flow cytometry study (Invitrogen™ Attune™ NxT, Thermofisher Scientific, Singapore, Malaysia) confirmed the presence of 90% GFP-tagged cells. Selected cells were then expanded until Passage 3 in order to obtain the number of cells necessary for their characterization and for seeding the patches.

2.3. Characterization of ovine UC-MSC

Characterization of UC-MSCs included a proliferation analysis until passage 5, a phenotype analysis by flow cytometry and an analysis of their multipotency. Doubling time (T_D) was calculated for each passage according to the following equation: $T_D = \ln 2 \times t / [\ln (N_f) - \ln (N_i)]$ (t: time period, N_f: number of viable cells at the end of passage, N_i: number of plated cells) (21). The phenotype analysis was performed on cells at passage 3 to assess MSCs membrane antigens expression according to the International Society for Cellular Therapy definition (CD29, CD73, CD90, CD105, CD45) and antigens expression usually analyzed in the study of ovine MSCs (CD31, CD44, CD166) [21-24] (details on antibodies providers: additional table 1). Samples of 1X10^5 cells were washed twice in PBS. Antibodies were incubated with the cells for 30 min at 4°C. The samples were analyzed directly with the

Invitrogen™ Attune™ NxT flow cytometer (Thermofisher Scientific, Singapore, Malaysia). Unstained cells served as negative control for background fluorescence. At least $1x10^4$ events were measured per sample. DATA was analyzed with Invitrogen™ Attune™ NxT Software.

Adipogenic and osteogenic differentiations of isolated cells were analyzed at passage 3. UC-MSCs were incubated in the differentiation induction medium during 21 days at 37°C with 5% CO_2. Osteogenic differentiation induction medium was composed of: DMEM high glucose (Cytiva, South Logan, USA), FBS 10 % (Biowest, Nuaille, France), dexamethasone 10^{-7} M (Sigma, Saint Louis, USA), ascorbic acid 50 µg/mL (Sigma, Saint Louis, USA), inorganic phosphate 0,5 mM (Sigma, Saint Louis, USA), antibiotic-antimycotic 1X (Gibco, Life technologies, Grand Island, USA). After the incubation period, cells were fixed in 4% paraformaldehyde (Electron Microscopy Sciences, Hatfield, USA) for 10 min, washed in Dulbecco's phosphate-buffered saline (PBS, Eurobio, Les Ullis, France) and stained with Alizarin red 2% pH 4,2 (Sigma, Saint Louis, USA) for 15 minutes. Cells were observed under an inverted microscope in order to detect a red coloration of the calcium matrix. Adipogenic differentiation induction medium was composed of: DMEM low glucose (Cytiva, South Logan, USA), FBS 20% (Biowest, Nuaille, France), dexamethasone 10^{-6} M (Sigma, Saint Louis, USA), indomethacin 60 µM (Sigma, Saint Louis, USA), isobuthylmethyxanthin 0,5 mM (Sigma, Saint Louis, USA), insulin 5 µg/mL (Lilly, Fegersheim, France), antibiotic-antimycotic 1X (Gibco, Life technologies, Grand Island, USA). After the incubation period, cells were fixed in 4% paraformaldehyde (Electron Microscopy Sciences Hatfield, USA) for 10 min and washed in PBS. The cells were then incubated with 60% isopropanol (GPR Rectapur, VWR Biochemicals, Saint Louis, USA) for 5 minutes in order to permeabilize their membrane. Finally, cells were stained with Oil red (Sigma, Saint Louis, USA) and observed under an inverted microscope in order to detect pink colored lipid vacuoles.

2.4. Preparation of the UC-MSCs fibrin patch

GFP-tagged UC-MSCs at passage 3 were seeded into a fibrin patch formed by combining fibrinogen (20 mg/mL) with thrombin (4 NIH units/mL) from the EVICEL® kit (Ethicon, NJ, USA) as previously described [25]. Each patch was seeded with UC-MSCs from the same donor, since cells from different donors were not pooled. The fibrinogen solution was composed of 70% complete medium and 30% fibrinogen, and the thrombin solution, of 99.6% complete medium and 0.4% thrombin. Sixteen million GFP-labelled cells were suspended in 1800 µL of the fibrinogen solution in a 21.5 cm^2 Petri dish (Corning, Tewksbury, USA) containing a layer of solid agarose gel. The same volume of thrombin solution was rapidly added to the fibrinogen-cell mix as 25 µL droplets. The polymerization of this solution was obtained at 37°C within 10 minutes. After verification of proper polymerization, 4 mL of complete medium was added to each Petri dish and the patches were incubated at 37°C until their *in vivo* graft. Acellular patches were produced using the same technique, without adding cells to the fibrinogen solution.

To evaluate the survival and migration capacity of the cells within the patch *in vitro*, a study was performed using BIOSTATION ImQ (Nikon, Tokyo, Japan) for 48 hours. UC-MSCs patches sections (10 µm) were also observed under fluorescent microscopy using the Panoramic Digital Slide Scanner 250 Flash III (3DHistech Ltd) to evaluate the cells distribution into the patch mesh and the cells survival at 2 days and 4 days after their seeding.

2.5. MMC defect creation and repair in the ovine model

Pregnant ewes arrived at the housing facility one week prior to the first surgical intervention and had free access to food and water except for the 24-hour period directly preceding surgery. The MMC creation and repair were performed under general anesthesia using an induction with intravenous thiopental 10 mg/kg (Panpharma, Beignon, France), endotracheal intubation and maintenance with isoflurane 2%, (Axience, Pantin, France) with

sterile conditions. For all interventions, ewes were administered nalbuphine (0.2 mg/kg, intramuscular, Mylan, Saint Priest, France) for pre and postoperative pain control. Intravenous cefamandole was administered as preoperative surgical prophylaxis, and cefamandole (Panpharma, Beignon, France) was also instilled into the amniotic fluid before hysterotomy closure.

The MMC defect creation was performed at 75 days of gestation. Each ewe underwent laparotomy and hysterotomy followed by creation of the MMC defect. Briefly, the lumbar skin and the paraspinal muscles were removed to expose the spinal cord. A complete laminectomy from L1 to L5 was performed. The dorsal portion of the dura was removed between the origins of the dorsal roots from L1 to L5. The fetus was then returned to the uterine cavity, and intrauterine warm lactated Ringer's solution was administrated before hysterotomy closure, using a continuous running suture (2-0 Vicryl®). Maternal abdominal aponeurosis and skin were then closed using 1 MonoPlus® and 2 Filapeau® running sutures, respectively.

The MMC defect repair was performed at 90 days of gestation (Additional fig.1). Fetuses were randomly assigned to the UC-MSCs patch group or the acellular patch one. After removal of the fibrinous material covering the spinal cord using microsurgical scissors, the UC-MSCs patch or the acellular patch was placed over the exposed spinal cord and the skin was closed over the patch, using 2-0 Vicryl® stiches. Intrauterine warm lactated Ringer's solution was administrated before hysterotomy closure, reintegration of the uterus and closure of the maternal wall.

2.6. Neurological examination at birth

Lambs were delivered by cesarean section at 142 days of gestational age (full term: 145 days). During cesarean sections, maintenance of general anesthesia was achieved by using propofol alone (without isopropanol) to limit the risk of respiratory distress in lambs at birth. Lambs' motor functions were assessed using the sheep locomotor rating (SLR) scale developed by Brown *et al*[26]. This scale provides an accurate assessment of motor

functions ranging from complete paraplegia with no joint movement (0/15) to normal locomotion (15/15). It is based on the study of hindlimb joint movements, ability to stand, to ambulate, to step and to walk over a bar. For each lamb, a 5-minute video was recorded at one hour of life in order to perform an evaluation of motor functions by a pediatrician specialized in physical medicine and rehabilitation, blinded to the type of prenatal management. The 24-hour motor function analysis was not possible in this study. During the first two hours of life, the tail movements and voiding abilities of the lambs were also recorded. The hind limbs of each lamb were examined for the presence of amyotrophy.

2.7. Histopathologic and immunohistochemical analysis

After two hours of observation, all lambs were sacrificed using a pentobarbital sodium intravenous perfusion via one of the umbilical veins (5 mL of Dolethal® 200 mg/mL). After gross examination of the lambs, the area of the MMC defect was removed “en bloc” (including the spine, spinal cord, subcutaneous tissue, and skin). The central part of the MMC defect (5mm of length) was cryopreserved and both extremities (15mm of length) were fixed in 10% formaldehyde. All the following organs were also harvested to detect the presence of potential tumors: brain, lungs, liver, spleen, intestines, colon.

Cross-sections (5µm) of paraffin embedded MMC defect were stained for histopathological analysis using Hematoxylin Erythrosin Saffron (HES). Spinal cord tissue area, large neurons count (neurons with a diameter of 30-70 µm in the ventral gray matter) and fibrosis thickness (distance between the spinal cord and the dermis) were analyzed in two cross-sections per animal, that were taken from the upper and lower areas closest to the center of the MMC defect. Slides images were acquired using the PANNORAMIC Digital Slide Scanner 250 Flash III (3DHistech Ltd). Spinal cord tissue area and fibrosis thickness were selected and calculated using CaseViewer 2.2.1 software (3D Histech Ltd.). Large neurons density was calculated dividing the number of neurons by the gray matter area.

Immunohistochemical stainings were performed on 5µm cross-sections of the cryopreserved central zone of the MMC defect, to study the survival and localization of the UC-MSCs. Cross-sections were incubated for 30 minutes with 10% bovine serum albumin (BSA) to saturate non-specific antigenic sites. They were then incubated with 1/200 diluted anti-GFP primary antibody (Anti-TurboGFP(d) antibody, Evrogen, Moscow, Russia) for 60 minutes in a dark humid chamber at ambiant temperature. After rinsing with PBS, sections were incubated with 1/50 diluted secondary antibody (Goat anti-Rabbit Antibody DyLight® 680 Conjugated, Bethyl laboratories, Montgomery, USA) for 30 minutes in a dark humid chamber at ambiant temperature. After a new rinse with PBS, DAPI solution was instilled before a lamella was applied. We also studied expression of the neuroprotective factors Brain-Derived Neurotrophic Factor (BDNF) and Nerve Growth Factor (NGF). Cross-sections were incubated for 30 minutes with 10% BSA and incubated with 1/200 diluted anti-BDNF (BDNF Polyclonal Antibody, Cy5 Conjugated, Bioss Antibodies, Woburn, USA) or 1/200 diluted anti-NGF (NGF beta Polyclonal Antibody, Cy5 Conjugated, Bioss Antibodies, Woburn, USA) antibody for 60 minutes in a dark humid chamber at ambiant temperature. After rinsing with PBS, a DAPI solution was instilled before a lamella was applied. Anti-BDNF and anti-NGF antibodies were tested on cortex of healthy lambs upstream in order to verify their performance in sheep and to establish the most appropriate dilution. BDNF and NGF fluorescence After converting color images to grayscale, fluorescent intensities were quantify using ImageJ J 1.51 software.

2.8. Statistical analysis

The SLR scores, spinal cord areas, large neurons densities, measurements of fibrosis, BDNF and NGF fluorescence levels in each group were reported as median with 25–75% interquartile range (IQR) and compared using the Mann–Whitney U-test. Presence of tail movements, spontaneous voiding, amyotrophy, and spinal cord destruction were compared using the chi square (χ^2) test. All analyses were completed using GraphPad Prism 9.0.0 software (GraphPad Software, LLC) with significance set at $p < 0.05$.

3. Results

3.1. Ovine UC-MSCs patch

A mean of $2.76x10^6$ UC-MSCs were isolated from each umbilical cord in a mean period of 11 days. The mean UC-MSCs doubling time at passages 2, 3, 4, and 5 were 51.3 ± 7.8, 49.5 ± 15.1, 58.3 ± 13.8 and 73.1 ± 21.4 hours, respectively. All isolated UC-MSCs were fusiform and adherent to the plastic. Immunophenotypic characterization at passage 3 showed that isolated UC-MSCs were positive for MSC markers CD73, CD90, CD105, CD166, CD29, CD44, and negative for hematopoietic marker CD45 and endothelial marker CD31 (fig.1A). UC-MSCs were shown to differentiate along osteogenic and adipogenic lineages (fig.1B). UC-MSCs and acellular patches were easily produced. Their flexibility and their thickness of about 2 mm allow a convenient handling during repair surgeries (fig.2A). UC-MSCs patches study in biostation and under fluorescence microscopy demonstrated the *in vitro* survival of the cells for at least four days and their ability to adhere and migrate within the fibrin mesh (fig.2B).

3.2. Clinical evaluation

MMC defect was created in 20 fetuses at a median gestational age of 75 days. At 90 days of gestation, 10 fetuses underwent an MMC repair using an UC-MSCs patch and 10, using an acellular patch. The overall survival rate was 60% and six lambs in each group were born alive at 142 days of gestation.

There was no significant difference in the SLR score median between the two groups but the number of lambs with a score lower than 3 was significantly higher in the control group (table 1). In the UC-MSCs group, the SLR score was 6 for two lambs (33%), 4 for one (17%), and lower than 3 for three (50%) (fig.3). In the control group, all lambs had a SLR score lower than 3 (fig.3). No lambs in the control group had spontaneous tail movements, whereas these were observed in 5/6 lambs (83%) in the UC-MSCs group (*p=0.003*). Hind

limb amyotrophy was present in all lambs in the control group, and in 3/6 (50%) of the lambs in the UC-MSCs group. Spontaneous voiding was observed in 3/6 (50%) of the lambs in the UC-MSCs group and none of the control lambs.

3.3. Histological and immunohistochemical examinations

All lambs had normal macroscopic examination of brain structures and especially, of the hindbrain.

All lambs in both groups presented a complete epidermis and dermis healing of the MMC lesion. We observed neo-cartilage for 2/6 (33%) lambs of the UC-MSCs group versus none of the control group (p=0.12). A complete healing of the dura was observed for all the lambs of the UC-MSCs group and 2/6 (33%) of the control group (p=0.06). The thickness of fibrous tissue between the spinal cord and the dermis was more significant in the control group than in the UC-MSCs group (2624 µm vs 1269 µm, p=0.015) (table 2). We also observed fibrous tissue surrounding the spinal cord in both groups, but this fibrosis was thicker in the control lambs than in those of the UC-MSCs group (588 µm vs 175 µm, *p=0.024*).

Although the spinal cord area was not statistically significant between both groups, the median grey matter area significantly differs with a median grey matter area of 2.4 mm^2 in the UC-MSCs group compared to 0.8 mm^2 in the control group (*p=0.02*) (fig.4). Large neurons density was significantly higher in the UC-MSCs group than in the control group (19.3 versus 1.6 neurons/mm^2, *p=0.03*) (table 2).

Immunohistochemistry study of the MMC area demonstrated the presence of a few GFP-tagged cells in 3/6 (50%) lambs of the UC-MSCs group (additional fig.2). The sparsely observed cells were located in the dermis and in a fibroid structure covering the spinal cord, evocative of a residual patch. No GFP-tagged cells were found in the spinal cord. Spinal cord BDNF fluorescence levels were higher in UC-MSCs group with no statistically significant difference (table 2). No difference was observed in NGF fluorescence levels between the two groups (table 2).

No tumors were observed on macroscopic and microscopic examinations of the brain, lungs, liver, spleen, and intestines of any of the lambs in both groups.

4. Discussion

4.1. Efficiency of UC-MSCs as an adjuvant therapy in prenatal MMC surgical repair

Our results demonstrated that fetal repair of MMC using allogenic UC-MSCs patch in the ovine model provides a partial improvement in neurological functions at birth. The clinical benefit seems to be both motor and urinary. These results are consistent with those from Kabagambe *et al.* [27], reporting the surgical grafting of human placental mesenchymal stromal cells (pMSCs) in the same model as ours. pMSCs were used at passage 6, seeded on a 12 cm^2 porcine small intestinal submucosa-derived extracellular matrix at a density of 42,000 cells/cm^2 (total of 504,000 pMSCs). They observed a median SLR score of 15 (4-15) in the pMSCs group and 6 (3-15), in the control group, with 63% of lambs able to ambulate independently and walk over an obstacle in the pMSCs group. The same group studied the impact of cell dose and the donor-dependent effect on motor functions at birth [28,29]. They demonstrated that there was no difference between a density of 42,000/cm^2 and 300,000 cells/cm^2 (12cm^2 matrix) on the SLR score [28]. Their experimentation with three cell populations from different donors shows similar SLR scores between the three groups, but a rate of ambulation that appears to be lower for one of the donors [29]. This suggests that it could be interesting to use a pool of cells from different donors in order to minimize cells properties variability.

Despite a substantially higher number of grafted cells and the choice of an allogeneic graft rather than a xenogeneic graft, we observed less satisfying results regarding the motor function improvement compared to Kabagambe's results [27]. This could be explained by several hypotheses. The main hypothesis is that our surgical technique was not exactly

similar and that we whether induced spinal cord injuries when excising the dura or more severe spinal deformities, which could affect neurological prognosis of the lambs. Vanover *et al.* demonstrated that there was a negative correlation between SLR score and spinal deformity induced by laminectomy performed during surgical MMC creation [30]. These authors also demonstrated that the size of the lamina remaining portion correlates with spinal deformity at birth. There are no specific guidelines to perform the laminectomy of the MMC surgical ovine model. It is therefore possible that differences in our surgical technique resulted in more severe spinal deformities in our cohort compared to those of Farmer's group [27-29]. Motor evaluation described in Brown's score is performed at birth, but also at 24 hours of life, after the animal adaptation postnatal environment. Brown *et al.* reported that newborn lambs often demonstrated weakness and lacked coordination shortly after birth and that motor function improved significantly within 24 hours. Assessment of motor function shortly after birth is a limitation of our study and this could explain why our control lambs have lower scores than those in Kabagambe's study [27]. Unfortunately, at the time of the study we did not have the human and financial resources to monitor the lambs for 24 hours. Another hypothesis to explain our lower SLR scores compared to the ones reported by Kabagambe *et al.* could be that human placental MSCs have greater potential than ovine UC-MSCs in nervous tissue repair.

Our results demonstrated that ovine UC-MSCs, grafted in a sheep model of MMC, provided gray matter and neuronal preservation. These results are consistent with Farmer Group's findings. In their four studies, they showed that grafting human placental MSCs promoted neuronal preservation and that this effect appears to be donor-dependent and greater for higher cell densities [27-29,31]. The exact mechanisms to explain the benefit of MSCs on spinal cord preservation have not yet been fully demonstrated. The most likely hypothesis is that the cells act through their paracrine properties rather than a differentiation into neurons. In our study, we demonstrated a cell survival time of at least 52 days as we observed GFP-tagged cells in 50% of the cases at the MMC lesion level. UC-MCSs were located in the dermis or in the residual patch, but never integrated into the spinal cord. This

supports the hypothesis that UC-MSCs do not differentiate into nerve cells. We also observed a tendency toward higher BDNF expression in the spinal cord of the UC-MSCs lambs. These results are consistent with those of Li *et al.* who experimented allogeneic bone marrow-MSCs injections in the retinoic-induced MMC rat model and observed a higher BDNF and NGF expressions in the spinal cord of the treated animals. Finally, several studies conducted in animal models of spinal cord injury have indicated increased expression of many growth factors and neurotrophic factors in the spinal cord of animals treated with UC-MSCs [15,17,32].

Our study is the first to demonstrate the interest of UC-MSCs to prevent from fibrosis development at the MMC scar level, after prenatal repair. Brown *et al.* reported a decrease in spinal cord adhesions in the ovine model of MMC treated with autologous amniotic membrane's grafting. Based on our results, it is possible that this effect was related to the presence of MSCs in amniotic membrane. This anti-fibrotic effect is particularly interesting considering the high risk of tethered spinal cord syndrome after prenatal and postnatal MMC surgery which may be associated with a worsening of motor and sphincter functions [6,33,34]. Thus, the use of UC-MSCs as an adjuvant therapy could have a benefit both for prenatal surgery, but also for postnatal surgery and in broader indications than the treatment of MMC. The anti-fibrotic effect of MSCs has been demonstrated by numerous experimental studies and these cells are currently used in clinical research in several pathologies such as hepatic cirrhosis or scleroderma, for this particular effect [35].

4.2. Safety of UC-MSCs patch in prenatal MMC surgical repair

Despite a large number of transplanted cells, we did not observe any tumors in lambs at birth, 52 days after UC-MSCs grafting. These results are consistent with all studies conducted in MMC animal models that have experimented MSCs from various sources and administration routes [27-29,31,36-38]. Two studies reporting the use of UC-MSCs patches

in traumatic spinal cord injury in humans are also reassuring, with no serious side effects in the year following transplantation [19,20]. Finally, a recent meta-analysis including 2696 patients confirmed the absence of severe complications related to MSC therapy as malignancy, infection, organ failure, death [39].

Evicel® is a second-generation fibrin sealant indicated in surgery as adjunctive hemostatic therapy, and suture line sealing in dura mater closure. The safety of EVICEL® has been demonstrated in experimental and clinical studies [40-43]. Besides, Evicel® is the only fibrin sealant with Marketing Authorization in neurosurgery.

5. Conclusions

Our results strengthen those of Farmer *et al.* in demonstrating the benefit of using MSCs as adjunctive treatment for MMC fetal surgery. However, UC-MSCs availability is probably higher than that of early gestation placental cells. Cord blood banks already exist in many countries, and maternity hospitals that provide cord blood also provide umbilical cords [44].

Conflicts of Interest

The authors declare no conflict of interest.

Funding

This work was supported by funding from the Fondation de l'Avenir (Grant #AP-RMA-18-028).

Acknowledgements

We thank the "Fer à Moulin" School of Surgery of Paris, and particularly Josette Legagneux, for their investment in this project's organization. We thank Olivier Trassard (INSERM UMS44), in charge of the "High-Throughput Digital Slides Acquisition and Analysis Platform": Paris Saclay University, Kremlin Bicêtre Hospital, Department of Pathology, Le Kremlin-Bicêtre, France. We thank Katia Posseme and Olivier Morassi for their valuable support in histological analyses. We thank the Technological Core Facility of the Saint-Louis Research Institute (Paris, France) for their support.

References

1. Adzick NS, Thom EA, Spong CY, Brock JW 3rd, Burrows PK, Johnson MP, et al. A randomized trial of prenatal versus postnatal repair of myelomeningocele. N Engl J Med. 2011 Mar 17;364(11):993-1004.
2. Zamłyński J, Olejek A, Koszutski T, Ziomek G, Horzelska E, Gajewska-Kucharek A, et al. Comparison of prenatal and postnatal treatments of spina bifida in Poland--a non-randomized, single-center study. J Matern Fetal Neonatal Med. 2014 Sep;27(14):1409-17.
3. Moron AF, Barbosa MM, Milani H, Sarmento SG, Santana E, Suriano IC, et al. Perinatal outcomes after open fetal surgery for myelomeningocele repair: a retrospective cohort study. BJOG. 2018 Sep;125(10):1280-1286.
4. Möhrlen U, Ochsenbein-Kölble N, Mazzone L, Kraehenmann F, Hüsler M, Casanova B, et al. Benchmarking against the MOMS Trial: Zurich Results of Open Fetal Surgery for Spina Bifida. Fetal Diagn Ther. 2020;47(2):91-97.
5. Guilbaud L, Maurice P, Lallemant P, De Saint-Denis T, Maisonneuve E, Dhombres F, et al. Open fetal surgery for myelomeningocele repair in France. J Gynecol Obstet Hum Reprod. 2021;50(9):102155.
6. Houtrow AJ, Thom EA, Fletcher JM, Burrows PK, Adzick NS, Thomas NH, et al. Prenatal Repair of Myelomeningocele and School-age Functional Outcomes. Pediatrics. 2020;145(2):e20191544.
7. Macedo A Jr, Ottoni SL, Garrone G, Liguori R, Cavalheiro S, Moron A, et al. In utero myelomeningocoele repair and urological outcomes: the first 100 cases of a prospective analysis. Is there an improvement in bladder function? BJU Int. 2019;123(4):676-681.
8. Clayton DB, Thomas JC, Brock JW 3rd. Fetal repair of myelomeningocele: current status and urologic implications. J Pediatr Urol. 2020;16(1):3-9.
9. Mennan C, Wright K, Bhattacharjee A, Balain B, Richardson J, Roberts S. Isolation and characterisation of mesenchymal stem cells from different regions of the human umbilical cord. Biomed Res Int. 2013;2013:916136.

10. Nancarrow-Lei R, Mafi P, Mafi R, Khan W. A Systemic Review of Adult Mesenchymal Stem Cell Sources and their Multilineage Differentiation Potential Relevant to Musculoskeletal Tissue Repair and Regeneration. Curr Stem Cell Res Ther. 2017;12(8):601-610.
11. Guillot PV, Gotherstrom C, Chan J, Kurata H, Fisk NM. Human first-trimester fetal MSC express pluripotency markers and grow faster and have longer telomeres than adult MSC. Stem Cells. 2007 Mar;25(3):646-54.
12. Lu LL, Liu YJ, Yang SG, Zhao QJ, Wang X, Gong W, et al. Isolation and characterization of human umbilical cord mesenchymal stem cells with hematopoiesis-supportive function and other potentials. Haematologica. 2006 Aug;91(8):1017-26.
13. Dalous J, Larghero J, Baud O. Transplantation of umbilical cord-derived mesenchymal stem cells as a novel strategy to protect the central nervous system: technical aspects, preclinical studies, and clinical perspectives. Pediatr Res. 2012;71:4 Pt 2.
14. Teixeira FG, Carvalho MM, Sousa N, Salgado AJ. Mesenchymal stem cells secretome: a new paradigm for central nervous system regeneration? Cell Mol Life Sci. 2013 Oct;70(20):3871-82.
15. Hu SL, Luo HS, Li JT, Xia YZ, Li L, Zhang LJ, et al. Functional recovery in acute traumatic spinal cord injury after transplantation of human umbilical cord mesenchymal stem cells. Crit Care Med. 2010 Nov;38(11):2181-9.
16. Tian DZ, Deng D, Qiang JL, Zhu Q, Li QC, Yi ZG. Repair of spinal cord injury in rats by umbilical cord mesenchymal stem cells through P38MAPK signaling pathway. Eur Rev Med Pharmacol Sci. 2019 Aug;23(3 Suppl):47-53.
17. Wu LL, Pan XM, Chen HH, Fu XY, Jiang J, Ding MX. Repairing and Analgesic Effects of Umbilical Cord Mesenchymal Stem Cell Transplantation in Mice with Spinal Cord Injury. Biomed Res Int. 2020 Apr 4;2020:7650354.
18. Liu J, Han D, Wang Z, Xue M, Zhu L, Yan H, et al. Clinical analysis of the treatment of spinal cord injury with umbilical cord mesenchymal stem cells. Cytotherapy. 2013 Feb;15(2):185-91.

19. Xiao Z, Tang F, Zhao Y, Han G, Yin N, Li X, et al. Significant Improvement of Acute Complete Spinal Cord Injury Patients Diagnosed by a Combined Criteria Implanted with NeuroRegen Scaffolds and Mesenchymal Stem Cells. Cell Transplant. 2018 Jun;27(6):907-915.
20. Deng WS, Ma K, Liang B, Liu XY, Xu HY, Zhang J, et al. Collagen scaffold combined with human umbilical cord-mesenchymal stem cells transplantation for acute complete spinal cord injury. Neural Regen Res. 2020 Sep;15(9):1686-1700.
21. Adamzyk C, Emonds T, Falkenstein J, Tolba R, Jahnen-Dechent W, Lethaus B, et al. Different Culture Media Affect Proliferation, Surface Epitope Expression, and Differentiation of Ovine MSC. Stem Cells Int. 2013;2013:387324.
22. Rentsch C, Hess R, Rentsch B, Hofmann A, Manthey S, Scharnweber D, et al. Ovine bone marrow mesenchymal stem cells: isolation and characterization of the cells and their osteogenic differentiation potential on embroidered and surface-modified polycaprolactone-co-lactide scaffolds. In Vitro Cell Dev Biol Anim. 2010 Jul;46(7):624-34.
23. Khan MR, Chandrashekran A, Smith RK, Dudhia J. Immunophenotypic characterization of ovine mesenchymal stem cells. Cytometry A. 2016 May;89(5):443-50.
24. Tian Y, Tao L, Zhao S, Tai D, Liu D, Liu P. Isolation and morphological characterization of ovine amniotic fluid mesenchymal stem cells. Exp Anim. 2016 May 20;65(2):125-34.
25. Bellamy V, Vanneaux V, Bel A, Nemetalla H, Emmanuelle Boitard S, Farouz Y, et al. Long-term functional benefits of human embryonic stem cell-derived cardiac progenitors embedded into a fibrin scaffold. J Heart Lung Transplant. 2015 Sep;34(9):1198-207.
26. Brown EG, Keller BA, Pivetti CD, Sitkin NA, Wang A, Farmer DL, et al. Development of a locomotor rating scale for testing motor function in sheep. J Pediatr Surg. 2015 Apr;50(4):617-21.
27. Kabagambe S, Keller B, Becker J, Goodman L, Pivetti C, Lankford L, et al. Placental mesenchymal stromal cells seeded on clinical grade extracellular matrix improve ambulation in ovine myelomeningocele. J Pediatr Surg. 2017 Oct 12:S0022-3468(17)30654-1.

28. Vanover M, Pivetti C, Lankford L, Kumar P, Galganski L, Kabagambe S, et al. High density placental mesenchymal stromal cells provide neuronal preservation and improve motor function following in utero treatment of ovine myelomeningocele. J Pediatr Surg. 2019 Jan;54(1):75-79.
29. Galganski LA, Kumar P, Vanover MA, Pivetti CD, Anderson JE, Lankford L, et al. In utero treatment of myelomeningocele with placental mesenchymal stromal cells - Selection of an optimal cell line in preparation for clinical trials. J Pediatr Surg. 2020 Sep;55(9):1941-1946.
30. Vanover M, Pivetti C, Galganski L, Kumar P, Lankford L, Rowland D, et al. Spinal Angulation: A Limitation of the Fetal Lamb Model of Myelomeningocele. Fetal Diagn Ther. 2019;46(6):376-384.
31. Wang A, Brown EG, Lankford L, Keller BA, Pivetti CD, Sitkin NA, et al. Placental mesenchymal stromal cells rescue ambulation in ovine myelomeningocele. Stem Cells Transl Med. 2015 Jun;4(6):659-69.
32. Yang CC, Shih YH, Ko MH, Hsu SY, Cheng H, Fu YS. Transplantation of human umbilical mesenchymal stem cells from Wharton's jelly after complete transection of the rat spinal cord. PLoS One. 2008;3(10):e3336.
33. Zerah M, Kulkarni AV. Spinal cord malformations. Handb Clin Neurol. 2013;112.
34. Hudgins RJ, Gilreath CL. Tethered spinal cord following repair of myelomeningocele. Neurosurg Focus. 2004;16:2.
35. Rockel JS, Rabani R, Viswanathan S. Anti-fibrotic mechanisms of exogenously-expanded mesenchymal stromal cells for fibrotic diseases. Semin Cell Dev Biol. 2020;101.
36. Dionigi B, Ahmed A, Brazzo J 3rd, Connors JP, Zurakowski D, Fauza DO. Partial or complete coverage of experimental spina bifida by simple intra-amniotic injection of concentrated amniotic mesenchymal stem cells. J Pediatr Surg. 2015;50(1):69-73.

37. Shieh HF, Tracy SA, Hong CR, Chalphin AV, Ahmed A, Rohrer L, et al. Transamniotic stem cell therapy (TRASCET) in a rabbit model of spina bifida. J Pediatr Surg. 2019;54(2):293-296.
38. Shieh HF, Ahmed A, Rohrer L, Zurakowski D, Fauza DO. Donor mesenchymal stem cell linetics after transamniotic stem cell therapy (TRASCET) for experimental spina bifida. J Pediatr Surg. 2018;53(6):1134-1136.
39. Thompson M, Mei SHJ, Wolfe D, Champagne J, Fergusson D, Stewart DJ, et al. Cell therapy with intravascular administration of mesenchymal stromal cells continues to appear safe: An updated systematic review and meta-analysis. EClinicalMedicine. 2020;19:100249.
40. Hutchinson RW, Mendenhall V, Abutin RM, Muench T, Hart J. Evaluation of fibrin sealants for central nervous system sealing in the mongrel dog durotomy model. Neurosurgery. 2011;69(4):921-8.
41. Atkinson JB, Gomperts ED, Kang R, Lee M, Arensman RM, Bartlett RH, et al. Prospective, randomized evaluation of the efficacy of fibrin sealant as a topical hemostatic agent at the cannulation site in neonates undergoing extracorporeal membrane oxygenation. Am J Surg. 1997;173(6):479-84.
42. Chalmers RT, Darling Iii RC, Wingard JT, Chetter I, Cutler B, Kern JA, et al. Randomized clinical trial of tranexamic acid-free fibrin sealant during vascular surgical procedures. Br J Surg. 2010 Dec;97(12):1784-9.
43. Green AL, Arnaud A, Batiller J, Eljamel S, Gauld J, Jones P, et al. A multicentre, prospective, randomized, controlled study to evaluate the use of a fibrin sealant as an adjunct to sutured dural repair. Br J Neurosurg. 2015;29(1):11-17.
44. Magalon J, Maiers M, Kurtzberg J, Navarrete C, Rubinstein P, Brown C, et al. Banking or Bankrupting: Strategies for Sustaining the Economic Future of Public Cord Blood Banks. PLoS One. 2015 Dec 1;10(12):e0143440.

Figures legends

Figure 1. Ovine UC-MSCs characterization

A – Flow cytometry immunophenotyping of isolated cells from ovine umbilical cords at passage 3 ($1x10^4$ events were measured per sample). Ovine UC-MSCs expressed the markers CD29, CD90, CD166, CD73, CD44, and CD105. UC-MSCs were negative for hematopoietic and endothelial lineage markers CD45 and CD31.

B – Directed differentiation of UC-MSCs demonstrated multipotency toward osteogenic and adipogenic cell lineages.

Figure 2. Ovine UC-MSCs patch

A – Picture of a UC-MSCs patch

B – Images extracted from a a UC-MSCs patch time lapse imaging in a BIOSTATION ImQ imaging platform (Nikon) at 0, 24, 48, and 72 hours (same patch's area). Time lapse imaging was performed using a Plan Apochromat 40X N.A. 0,8 Ph objective, an additional lens 0.5X (Final magnification 20X) and a Nikon DS-Qi1Mc black and white camera. Images were acquired in phase contrast with the Biostation Im software (v2,.21) at of rate of 6 images/hours over a period of 72h under optimal cell culture conditions (5% CO2, 95% H2O saturation, 37°C) (Scale bar: 100 µm).

Figure 3. Sheep Locomotor Rating scores in UC-MSCs and control groups (median values with interquartile range).

Figure 4. Histological analysis of the MMC defect after HES staining

A – Cross-section of the MMC defect in a lamb from the UC-MSCs group showing complete skin healing, presence of neocartilage, complete dura healing, and partial destruction of the spinal cord posterior horns (scale bar: 2000 µm).

B – Magnification of the spinal cord visualized in image A (scale bar: 1000 µm).

C – Cross-section of the MMC defect in a lamb from the UC-MSCs group showing complete skin healing, subcutaneous fibrosis and fibrosis surrounding the spinal cord, as well as significant destruction of the spinal cord (scale bar: 2000 µm).

1. epidermis
2. dermis
3. fibrosis
4. neocartilage
5. residual patch
6. spinal cord
7. dorsal root ganglion
8. vertebral body
9. dura mater
10. pia mater
11. ependymal canal
12. large neurons
13. fibrose is surrounding the spinal cord

Additional Figure 1. Representative photographs of the surgical MMC repair using an UC-MSCs patch at 90 days of gestation.

A – aspect of the MMC defect at 90 days of gestation

B – removal of the fibrin layer, covering the spinal cord

C – placement of the UC-MSCs patch on the defect

D – skin suture over the UC-MSCs patch using separate stitches

Additional Figure 2. Immunohistochemical analysis of the spinal cord of a lamb from UC-MSCs group

A – 5 µm section through the epidermis, dermis, residual patch and part of a spinal cord posterior horn.

B – Magnification of an area of the dermis showing the presence of a few sparse GFP-tagged cells, in red GFP was revealed with a primary anti-Turbo GFP antibody and a red secondary antibody, DyLight® 650 conjugated).

C- Magnification of a part of the residual patch showing the presence of one GFP-tagged cell.

D - Positive control: 5 µm section of the UC-MSCs patch analyzed according to the same protocol (primary anti-Turbo GFP antibody and a red secondary antibody, DyLight® 650 conjugated).

Table 1. Postnatal neurological examinations in the two groups

Outcome		**UC-MSCs** *n = 6*	**Controls** *n = 6*	**p-value**
SLR score [min-max] (/15)		3 [0 - 6]	1 [0 - 2]	*0.249*
SLR score	< 3	3 (50%)	6 (100%)	*0.046*
	3 – 5	1 (17%)	0	*0.296*
	> 5	2 (33%)	0	*0.121*
Tail movements		5 (83%)	0	*0.003*
Amyotrophy		3 (50%)	6 (100%)	*0.046*
Spontaneous voiding		3 (50%)	0	*0.046*

SLR: sheep locomotor rating

Table 2. Histologic analysis in the two groups

Outcome	**UC-MSCs** *n = 6*	**Controls** *n = 6*	p-value
Spinal cord area (*mm^2*)	4.8 [4.5 – 8.8]	2.2 [0 – 4.8]	*0.177*
Grey Matter area (*mm^2*)	2.5 [1.9 – 5.1]	0.8 [0 – 1.6]	*0.024*
Large neuron density (*nb neurons/mm^2 of gray matter*)	19.3 [17.1 – 27.5]	1.6 [0 – 5.0]	*0.002*
Thickness of fibrosis around the SC *(µm)*	175 [137 – 281]	588 [529 – 797]	*0.024*
Thickness of fibrosis between SC and dermis *(µm)*	1269 [1200 – 1863]	2624 [2239 – 2660]	*0.015*
BDNF fluorescence level	39.6 [35.5 – 42.2]	29.9 [24.6 – 34.0]	*0.058*
NGF fluorescence level	23.8 [21.2 – 28.0]	23.5 [21.9 – 27.6]	*0.898*

SC: spinal cord, BDNF: Brain-Derived Neurotrophic Factor, NGF: Nerve growth factor

Additional table

Additional Table 1 – Antibody providers

Antibodies		**Provider**
CD29	PE mouse anti-human CD29	Life Technologies, Thermo Fisher, Bleiswikj, Netherlands
CD31	Mouse anti-sheep CD31 FITC	Bio-Rad, Kidlington, UK
CD44	Mouse anti-sheep CD45 FITC	Bio-Rad, Kidlington, UK
CD45	Mouse anti-sheep CD44 FITC	Bio-Rad, Kidlington, UK
CD73	Rat anti-mouse CD73 PE	BD Pharmigen, San Diego, CA, USA
CD90	Mouse anti human CD90 PE	BD Pharmigen, San Diego, CA, USA
CD105	Rat anti-mouse CD105 PE	BD Pharmigen, San Diego, CA, USA
CD166	Mouse anti-human CD 166 PE	BD Pharmigen, San Diego, CA, USA

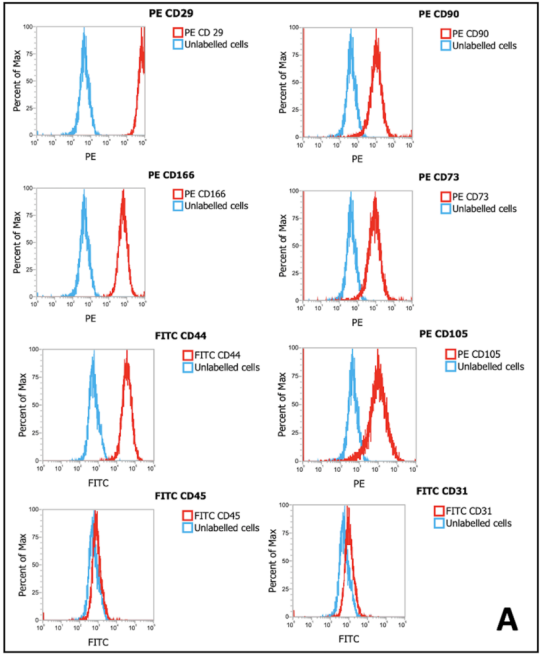
PE CD29
PE CD 29
Unlabelled cells
PE CD90
PE CD90
Unlabelled cells
PE CD166
PE CD166
Unlabelled cells
PE CD73
PE CD73
Unlabelled cells
FITC CD44
FITC CD44
Unlabelled cells
PE CD105
PE CD105
Unlabelled cells
FITC CD45
FITC CD45
Unlabelled cells
FITC CD31
FITC CD31
Unlabelled cells
Percent of Max
PE
FITC
A

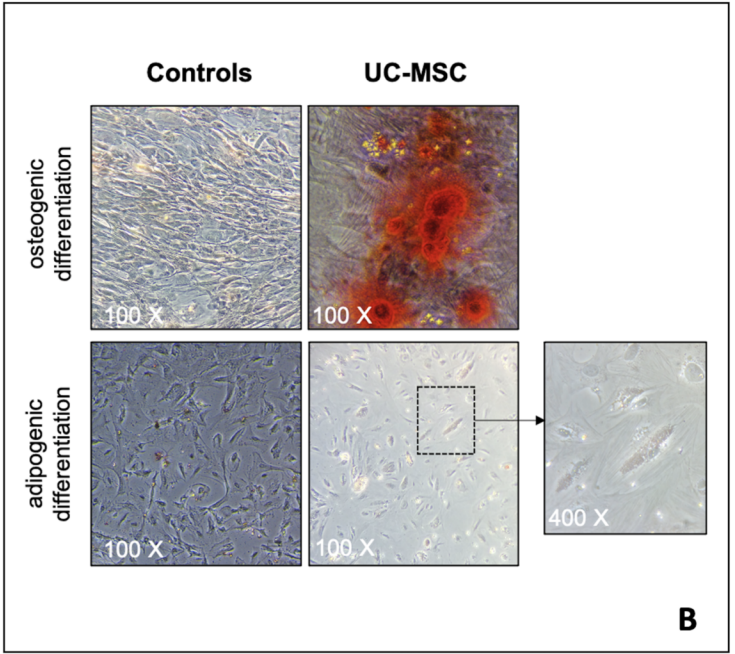
Controls
UC-MSC
osteogenic differentiation
adipogenic differentiation
100 X
100 X
100 X
100 X
400 X
B

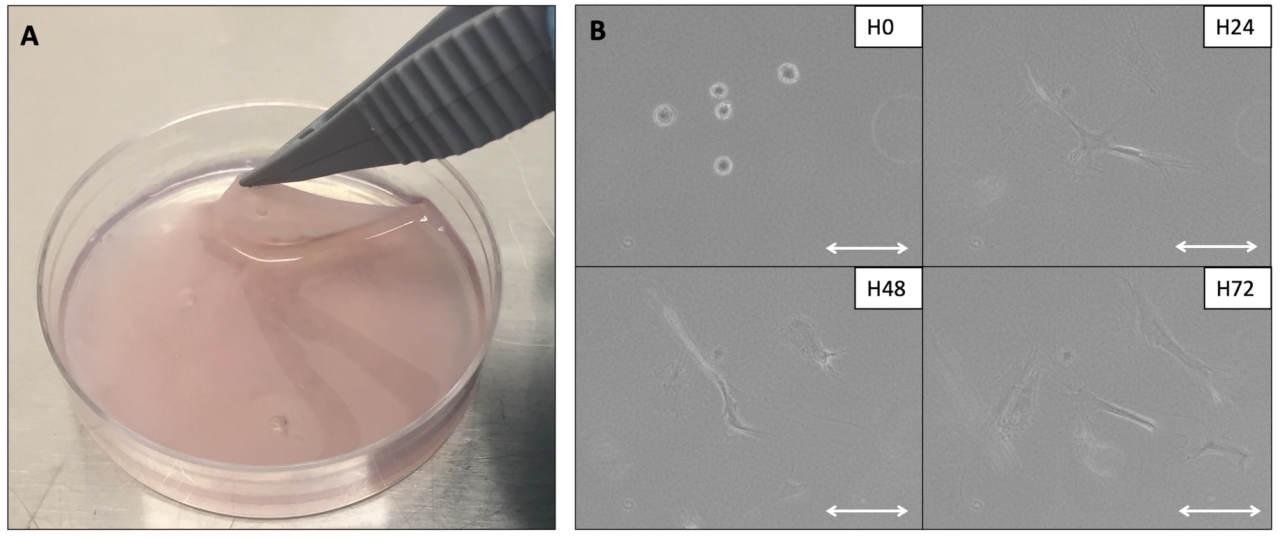
A
B
H0
H24
H48
H72

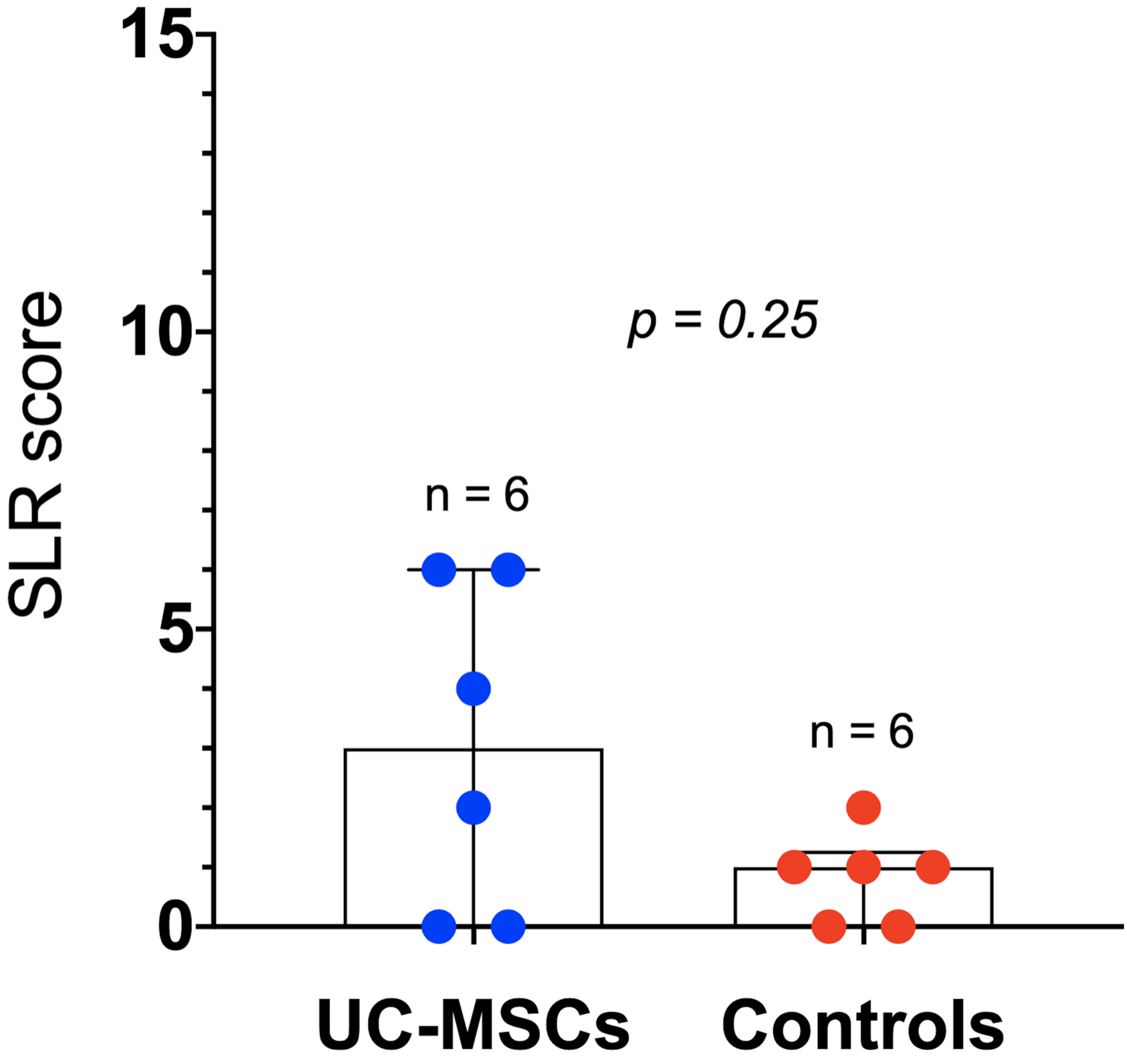
15
10
5
0
SLR score
p = 0.25
n = 6
n = 6
UC-MSCs
Controls

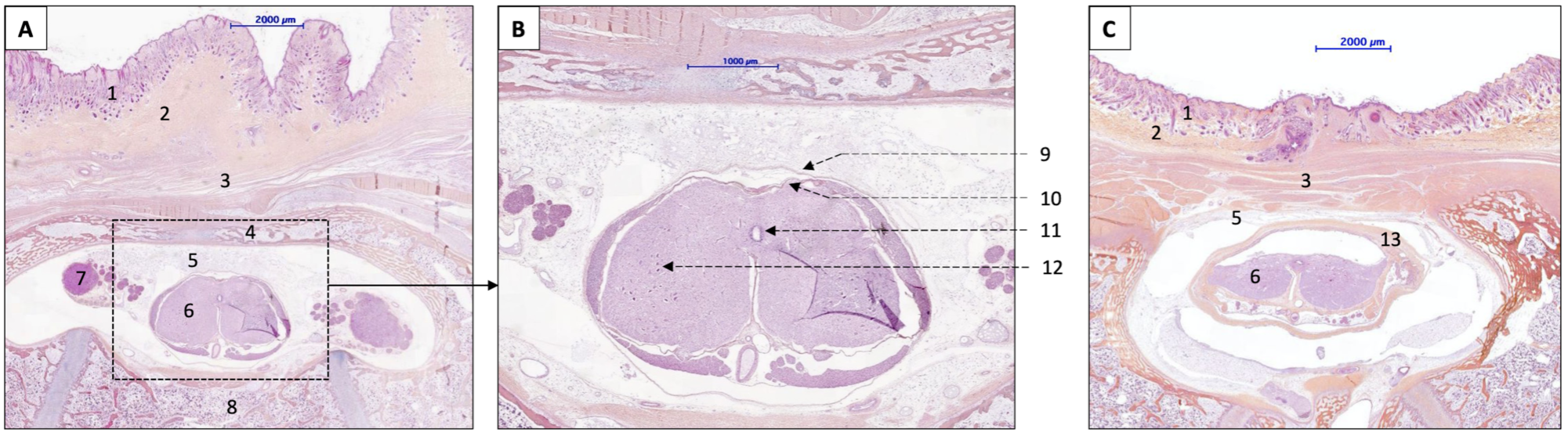
A
2000 µm
1
2
3
4
5
6
7
8
B
1000 µm
9
10
11
12
C
2000 µm
1
2
3
5
6
13